



Contents lists available at ScienceDirect

Journal of King Saud University – Science

journal homepage: www.sciencedirect.com

Original article

Antimicrobial, anti-melanogenesis and anti-tyrosinase potential of myco-synthesized silver nanoparticles on human skin melanoma SK-MEL-3 cells



S. Himalini^a, V. Uma Maheshwari Nallal^a, M. Razia^{a,*}, Sasikala Chinnapan^b, Murugesan Chandrasekaran^{c,*}, Venkatalakshmi Ranganathan^d, Mansour K. Gatasheh^e, Ashraf Atef Hatamleh^f, Fatimah S Al-Khattaf^f, S. Kanimozhi^g

^a Department of Biotechnology, Mother Teresa Women's University, Kodaikanal 624101, Tamilnadu, India

^b Department of Pharmaceutical Biology, Faculty of Pharmaceutical Science, UCSI University Kuala Lumpur, Kuala Lumpur, Malaysia

^c Department of Food Science and Biotechnology, Sejong University, Gwangjin-gu, Seoul 05006, Republic of Korea

^d Faculty of Pharmaceutical Sciences, UCSI University, 56000 Cheras, Kuala Lumpur, Malaysia

^e Department of Biochemistry, College of Science, King Saud University, P.O. Box 2455, Riyadh 11451, Saudi Arabia

^f Department of Botany and Microbiology, College of Science, King Saud University, P.O. Box 2455, Riyadh 11451, Saudi Arabia

^g Department of Biotechnology, Bharath Institute of Higher Education and Research, Selaiyur, Chennai, India

ARTICLE INFO

Article history:

Received 20 November 2021

Revised 11 December 2021

Accepted 28 January 2022

Available online 3 February 2022

Keywords:

Mycosynthesis

AgNPs

Resistance

Kojic acid

Anti-melanogenic

SK-MEL-3 cells

ABSTRACT

Objectives: Mycosynthesis offers a benevolent alternative for the synthesis of Silver Nanoparticles (AgNPs) when compared to the conventional physical and chemical methods. Fungi secrete enormous amounts of proteins and enzymes that act as reducing and capping agents in AgNPs synthesis.

Methods: AgNPs were synthesized using extracellular fungal extract of *Fusarium incarnatum*. The reaction mixture was optimized using different parameters to obtain better yield. Anti-melanogenic activity of fungal extract, AgNPs and standard drug (Kojic acid) was evaluated against Human skin melanoma SK-MEL-3 cells. AgNPs were synthesized at 30 °C, pH 5 and 1 mM AgNO₃ concentration. Then optimization and the characterization were done by UV-Vis, FTIR, XRD, Zeta potential and H-TEM techniques.

Results: The average size of AgNPs was 10 nm and predominantly spherical in shape. Myco-synthesized AgNPs showed significant anti-melanogenic activity against human skin melanoma SK-MEL-3 cells with an IC₅₀ value of 17.70 µg/ml. The concentration of AgNPs required to inhibit SK-MEL-3 cells was lower than the concentrations of *F. incarnatum* extract and standard Kojic acid.

Conclusion: Spherical AgNPs with an average size of 4 nm were synthesized using fungal extract of *F. incarnatum*. Mycosynthesized AgNPs can be considered as effective anti-melanogenic agents owing to their impressive activity against skin melanoma.

© 2022 The Author(s). Published by Elsevier B.V. on behalf of King Saud University. This is an open access article under the CC BY-NC-ND license (<http://creativecommons.org/licenses/by-nc-nd/4.0/>).

1. Introduction

The domain of nanotechnology is one of the most active fields in modern material science study (Malik et al., 2014). Among the

metallic nanoparticles, AgNPs have significant applications in the field of bio-labelling, antimicrobial agents, filters as well as sensors (Kathiresan et al., 2009). They also have a major role in the medicine and biology field (Shankar et al., 2004). AgNPs are significant candidates for their solution of many medical issues owing to their chemical bio-compatibility, resistance to oxidation, inertness, and a wider array of antimicrobial activities (Prabhu and Poulouse, 2012). Similarly, metal-microbes interaction has important roles in many applications of biotechnology such as biomineralization and bioremediation fields (Sastry et al., 2004). AgNPs are not likely to generate drug-resistant microbial strains and effectively kill bacteria at very low concentrations (less than 1–10 µm) by acting as a disinfectant (Deshmukh et al., 2019). Bacterial DNA, proteins,

* Corresponding authors.

E-mail addresses: razia.bt@motherteresawomenuniv.ac.in (M. Razia), chandrub-dubio@gmail.com (M. Chandrasekaran).

Peer review under responsibility of King Saud University.



Production and hosting by Elsevier

<https://doi.org/10.1016/j.jksus.2022.101882>

1018-3647/© 2022 The Author(s). Published by Elsevier B.V. on behalf of King Saud University.

This is an open access article under the CC BY-NC-ND license (<http://creativecommons.org/licenses/by-nc-nd/4.0/>).

enzymes, and bacterial cell walls are known to be damaged by silver ions. AgNPs directly affect bacterial growth via intra-cycling with the cell wall, which damages metabolic response gradually (Azmath et al., 2016).

Research on the synthesis and characterization of AgNPs has increased extensively (Salem et al., 2015). The nanoparticles biosynthesis was carried out using a wide array of microorganisms such as algae, fungi and bacteria (Lalitha et al., 2013). Many microorganisms, both multicellular as well as unicellular are recognized to develop inorganic materials either extracellular or intracellular that reduce metallic ions (Thakkar et al., 2010). Biomass or extracellular materials from microorganisms are currently used for biotransformation of Silver ions to AgNPs (AbdelRahim et al., 2017). This type of biogenic fabrication of AgNPs postulate promising alternative offering advantages such as environment-friendly nature, easy scale-up for large-scale synthesis and most significantly, high temperature, pressure, and use of toxic chemicals has been avoided (Dutta et al., 2020). Myco-synthesized AgNPs are most ideal than bacteria and other unicellular organisms owing to their easy handling and capability of extracellular AgNPs synthesis (Kalishwaralal et al., 2008). Nanoparticles synthesized using fungal extract are more stable with better mono-disparity (Balaji et al., 2009). Recent research showed that optimization of temperature, time, pH, the concentration of Silver nitrate (AgNO_3) can facilitate the rapid synthesis of AgNPs using biological extracts (Veerasingam et al., 2011). Fungi of the *Fusarium* genus chiefly inhabit the soil environments that are rich in minerals and nutrients such as undisturbed forest soils (Himalini and Razia, 2019).

Skin is the human body's largest organ which acts as a barrier against physical, chemical, mechanical and biological stress. Melanocytes form the basal layer of the skin and are highly susceptible to mutations which later results in a highly invasive type of skin melanoma known as melanoma (Laikova et al., 2019). Melanoma is characterized by the robust and rapid proliferation of cancerous cells, invasion and migration followed by resistance to conventional therapies (Konstantinov et al., 2016). Although conventional therapies that include surgery, chemotherapy, radiation therapy and immunotherapy are practised to treat melanoma, the recurrence and mortality rate are very high. It is vital to postulate new strategies to improve the life expectancy of melanoma patients using effective treatments and affordable drugs (Rigel et al., 2010). Therefore, the present study focuses on the rapid and efficient extracellular biosynthesis of AgNPs using the fungal extract of *F. incarnatum* and to evaluate its biological applications that would propose them as promising candidates in the field of medicine and therapy.

2. Materials and methods

2.1. Mycosynthesis of AgNPs

F. incarnatum was isolated from Pine forest soil of Kodaikanal hills, Tamilnadu, India. The isolated *F. incarnatum* was used to synthesize AgNPs; fungal biomass was cultured aerobically in Potato Dextrose Broth (PDB) and incubated for 24 h at 30 °C. After 24 h, Whatman No.1 filter paper was used to filter the fungal biomass and transferred into a conical flask, thoroughly washed 2–3 times by using distilled water to remove the residual media part and other debris. This filtrate was utilized for further AgNP synthesis. 10 ml of fungal extract was mixed into 90 ml of (1 mM) AgNO_3 and incubated to reduce Silver ions. Later, the flask was placed on a rotary shaker which rotates at 120 rpm in dark conditions. The same procedure was followed throughout the optimization process.

2.2. Optimization of AgNPs

A high yield of nanoparticles can be achieved by optimization. By changing the physicochemical factors involved in their synthesis processes like concentration of pH, medium, temperature, incubation period nanoparticles' stability may be regulated. The reaction was monitored at various AgNO_3 (1–5 mM) concentrations and temperatures were kept at 30, 40, 50, 60, 70, 80 & 90 °C. Optimum concentration and temperature were noted down for optimizing the pH. Then pH of the reaction was maintained at 3, 5, 7, 9, 11, and 12. The aforementioned process was replicated to optimize the incubation period for monitoring the response at 2, 8, 12, 16, 20 and 24 h.

2.3. Characterization of AgNPs synthesized using *F. incarnatum* extract

Visual observations have shown the formation of the nanoparticle when colour turn dark brown from light white. Therefore, sampling of the reaction mixture was done at regular intervals to determine the absorption maxima using the UV–Vis spectroscope (UV-1800 Shimadzu, Japan) for the wavelength of 300–800 nm to provide additional confirmation. The AgNPs powder was mixed with Potassium bromide and the spectrum was recorded using a Perkin-Elmer spectrometer (Spectrum–One, U.S.A.) in the range of 4500–500 cm^{-1} . The structural analysis was done by powder X-ray Diffraction (Burker D8 advance XRD) method and the diffraction was measured in the 2θ range from 20° to 80°. The AgNPs samples were scanned in the 2 h ranges using Zetasizer Nano SZ-90 and, the spectral data were operated at a current of 40 mA and voltage of 40 kV. The particle size was measured using the HRTEM (TECNAI-10) technique by using drop-coating biosynthesized AgNPs solution on carbon-coated TEM grids (40 × 40 μm mesh size). The morphology, size, electron diffraction and crystalline nature were determined by the SAED pattern.

2.4. Antimicrobial activity of AgNPs

The antimicrobial activity of AgNPs was tested against selected bacterial strains such as (A) *B. subtilis* (MTCC-441) (B) *K. pneumonia* (MTCC-3384) (C) *S. aureus* (MTCC-737) and (D) *E. coli* (MTCC-448) obtained from Microbial Type Culture Collection (MTCC) Gene bank, Chandigarh, India. They were sub-cultured in nutrient broth for 24 h at 30 °C. The spread plate was prepared with nutrient agar and then synthesized AgNPs were added at different concentrations (5, 10, 15 and 20 μL), and incubated at 35 °C overnight. After 24 h incubation period, the inhibition zone (mm) was measured (Delgado et al., 2018).

2.5. Evaluation of invitro anti-melanoma activity of AgNPs

2.5.1. Cell culture maintenance

Human skin melanoma SK-Mel-3 cell lines have been bought from the Cell repository of NCCS (“National Centre for Cell Sciences”), Pune, India. The cell line was maintained in DMEM (“Dulbecco's Modified Eagle Media”), which was supplemented with 10% FBS (“Fetal Bovine Serum”). To avoid bacterial contamination, streptomycin (100 $\mu\text{g}/\text{ml}$) and Penicillin (100 U/ml), was poured into the medium. The medium containing cell lines was maintained at 37 °C in a humidified setting with 5% CO_2 (Rajendran et al., 2021).

2.5.2. In-vitro cytotoxicity assay (MTT)

The cytotoxicity of the AgNPs and standard Kojic acid was evaluated by MTT assay. The SK-MEL-3 cells were placed in 96 well plates, incubated in a 5% CO_2 environment for 24 h at 37 °C. Then the samples were washed with PBS (pH 7.4). Each well (100 μL)

well) contained, 0.5% 3-(4, 5-dimethyl-2-thiazolyl)-2, 5-diphenyl-tetrazolium bromide (MTT) with 4 h incubation. Anti-proliferative effects of *F. incarnatum* fungal extract (100–250 μg), optimized AgNPs (5–30 μg) and standard Kojic acid (5–30 μg) was added to respective wells and incubated for 24 h and the findings were presented as cell cytotoxicity ratio for SK-MEL-3 cells using MTT assay and were represented as a percentage of the control value (Birla et al., 2013).

2.5.3. Cellular Tyrosinase activity

SK-Mel-3 skin cells (105 cells/well) were put in 24-well plates in 300 μL of medium containing different quantities of *F. incarnatum* fungal extract (100–250 μg), optimized AgNPs (5–15 μg) and standard Kojic acid (5–15 μg) respectively to test cell tyrosinase activity, and incubated for two days. The sample-treated cells have been rinsed with (PBS) and lysed with 1% Triton X-100/PBS. 50 μL of cellular lysate to 2 mM L-tyrosine was added. This reaction was then incubated for 3 h in the dark conditions at 37 $^{\circ}\text{C}$ and the absorption was measured by the spectrophotometer at 490 nm (Sarkhail et al., 2017).

2.5.4. DNA fragmentation

Alkaline SCGE (single-cell gel electrophoresis) comet assay assessed DNA damage in the treated cells. A 1% LMPA (low melting point agarose) layer was equipped on microscopic slides. Subsequently, SK-MEL-3 (50 ml) cells were added into 0.5% LMPA of 200 ml. In the pre-coated slides, the suspension was added. Slides were dipped in cold lysis solution at pH 10 (100 mM EDTA, 2.5 M NaCl, 1% Triton X-100, 10 mM Tris pH 10, 10% DMSO) and for 60 min maintained at 4 $^{\circ}\text{C}$. The slides were positioned in the alkaline pH-13 electrophoresis buffer to enable denaturation of DNA and remained there for 25 min. Further, slides were moved to an electrophoresis tank with a new alkaline electrophoresis buffer and electrophoresis was done at field strengths of 1.33 V/cm at 4 $^{\circ}\text{C}$ for 25 min. For 5 min, the slides had been neutralized with 0.4 M Tris (pH 7.5) and 20 mg/ml EB had been used to stain. For the visualisation of DNA damage, an epifluorescent microscope with a barrier filter of 590 nm and an excitation filter of 510–560 nm was employed (Wozniak et al., 2004).

3. Results & discussion

3.1. Mycosynthesis of AgNPs using *F. incarnatum*

The AgNPs formation has been verified by the colour change from creamy white to dark brown as observed by visual observation in Fig. 1. The colour change is related to the surface plasma resonance (SPR) phenomenon of the AgNPs (Lee and Jun, 2019). Microbes capture metal ions from the fluid and convert them to the elemental form using their enzymatic activity in extracellular synthesis. The production of nanoparticles in microbes can occur in stress-free settings, such as when metal ions are present in the medium (Siddiqi et al., 2018).

3.2. Optimization studies of AgNPs

Environmental conditions immensely transform the metabolism as well as the growth of fungi. Culture settings have been identified as important components that have a direct impact on productivity and economic process.

3.2.1. Effect of different substrate concentration

The synthesis efficiency was evaluated using different concentrations of the substrates. The maximum efficiency in synthesizing AgNPs was observed at 1 mM concentration and the UV–Vis spec-



Fig. 1. (a) Control (*F. incarnatum* fungal extract) (b) Visible colour change observed due to reduction of silver ions to silver nanoparticles.

tra for maximum absorption was recorded at 447 nm. The results suggest that the concentration of the substrate and the enzymes/proteins of the fungal extract were proportional which resulted in the efficient synthesis of AgNPs. Results of low substrate concentrations demonstrated less efficient results owing to the inadequateness of the substrate when compared to the fungal proteins and enzymes involved in substrate reduction. Our results correlate with the results of Singh et al. (2014) who reported the optimum concentration to be 1 mM for the synthesis of AgNPs using endophytic fungi extract.

3.2.2. Effect of different temperatures

Temperature plays a crucial role in influencing the formation of AgNPs. Distinctive temperatures (30, 40, 50, 60, 70, 80 & 90 $^{\circ}\text{C}$) were used to determine the optimum temperature for the synthesis. The colour change occurred rapidly at 30 $^{\circ}\text{C}$ when compared to other temperatures. The maximum peak in the UV–Vis absorption spectra was observed at 426 nm. Results proposed that at a higher temperature the synthesis of AgNPs were less efficient which might be due to the denaturation of proteins and enzymes in the fungal extract at higher temperatures (Raheman et al., 2011). Contrastingly, in a study, aimed at optimizing AgNPs synthesized using *F. oxysporium* extract, 60 $^{\circ}\text{C}$ was determined as the optimum temperature characterized by efficient protein secretion from the fungal extract due to heat shock (Birla et al., 2013).

3.2.3. Effect of different Hydrogen ion concentrations (pH)

To determine the impact of pH on the synthesis process, AgNPs were synthesized at various pH and the absorption maximum was recorded. The neutral pH 7 showed a better synthesis of AgNPs. At acidic pH, the yield of AgNPs was very less, whereas in alkaline pH aggregation of the synthesized AgNPs was observed. Better synthesis without flocculation or aggregation of the AgNPs was observed at neutral pH. The absorption maximum was recorded at 437 nm. Hydrogen ion concentration has a strong influence on nanoparticle synthesis which influences enzyme production. Birla et al. (2013) reported that a better yield of AgNPs was obtained at alkaline pH using the fungal extract of *F. oxysporium*. Our results were consistent with those of Singh et al. (2014) who found that pH 7 was optimal for the synthesis of AgNPs utilising endophytic fungi *Peni-*

cillium sp. Results suggested that the stability and robust function of the proteins and enzymes in the filtrate act efficiently as reducing and capping agents at neutral pH (Ganachari et al., 2012).

3.2.4. Effect of the incubation period

By incubating the reaction mixture for various periods, the impact of incubation duration was evaluated. Although the colour change was visually visible from 2 h of the incubation period, 24 h was considered as the optimal incubation period since the absorption highest peak was observed as 440 nm at this time. The intensity of the reddish-brown colour was related to the mixture's incubation time directly, and the maximal decrease of silver ions was achieved after 24 h. A rise in the number of AgNPs may be attributed to the increase in absorbance and colour intensity with time (Othman et al., 2019).

3.3. Characterization of optimized AgNPs

3.3.1. UV-visible spectroscopic analysis of optimized AgNPs

Because of the reducing agents released into the solution by fungal extracts, the colour changed from light white to dark brown. UV-visible spectra confirmed this; when exposed to a particular wavelength of light, the NPs exhibited a unique surface phenomenon known as SPR (Surface Plasmon Resonance); As a result, each kind of NP was analysed using UV-Vis spectroscopy develops a specific peak (Zada et al., 2018). UV-Vis spectroscopy was used to monitor the AgNPs synthesis using *F. incarnatum* extract; the light absorption pattern of the fungal biomass was detected in the spectrum of 300–800 nm. Synthesized AgNPs showed a maximum absorption peak at 450 nm in Fig. 2(a). The conversion of silver ions into AgNPs was verified, and SPR peaks of metal nanoparticles were shown to be dependent on the shape, size of a particle, as well as reaction media. Comparable results were obtained by Ningnanagouda et al. (2013). Singh et al. (2014) who reported the absorption, peak of AgNPs to be between 400 and 450 nm.

3.3.2. FTIR spectroscopic analysis of optimized AgNPs

The potential interaction between Silver and bioactive compounds, which is responsible for the synthesis and stability of nanoparticles, were identified using FTIR analysis (Fig. 2b). The vibrations of the amide I and amide II bands of protein with N-H stretching were represented by the bands at 1325, 1520, and 3290 cm^{-1} , respectively, whereas the C-H stretching vibration were represented by the band at 2295 cm^{-1} . The bands at 1325, 1210 cm^{-1} , and 1055 cm^{-1} corresponded to aromatic and aliphatic

amine C-N stretching vibrations, respectively (Roy and Das, 2014). The results showed that in extracellular enzyme filtrate from fungal mycelia, protein molecules are engaged in AgNP reduction and stability through free amino groups or cytokine residues, as well as the electrostatic attraction of negatively charged carboxylate groups. Similarly, the FTIR results of AgNPs synthesized from endophytic fungi and *F. oxysporum* showed the presence of amine and protein functional groups.

3.3.3. XRD analysis of optimized AgNPs

The XRD pattern showed the crystalline nature of the optimized AgNPs (Fig. 3a). The particle size of synthesized AgNPs was calculated from the XRD data. The XRD pattern of the AgNPs corresponded to the FCC (Face-Centered cubic) structure of silver ions. Scherrer's equation was used to calculate the average particle size. The particle size varied between 2 and 10 nm and the average size was calculated as 4 nm. Roy and Das, reported the average size of AgNPs synthesized from *Aspergillus foetidus* extract to be 10.59 nm which demonstrated excellent antimicrobial activity. The average size of the AgNPs synthesized from *F. incarnatum* extract was smaller when compared to the above study report which may be due to the unique protein and enzymes that differ between fungi resulting in different reduction sizes.

3.3.4. Zeta potential analysis of optimized AgNPs

The biosynthesized AgNPs' zeta potential measurement revealed a single sharp peak between 40 and 0 mV, with the highest intensity at 19.9 mV, Fig. 3(b). Negatively charged moieties are found on the surface of the AgNPs that expanded in the medium, indicating that they are negatively charged. The particles' repulsion may be attributable to the negative values, which indicate that the particles are extremely stable. Low zeta potential values of particles indicated that there was no flocculation and no tendency for particles to combine because of repulsion forces (Ningnanagouda et al., 2013).

3.3.5. HRTEM and SAED determination of optimized AgNPs

To evaluate AgNPs particle size and morphology, HTEM measurements were calculated. The particles were generally spherical and no agglomerate was seen in the HTEM micrograph, Fig. 4(a). The AgNPs particle size synthesized using *F. incarnatum* extract ranged from 5 to 10 nm. The results of the H-TEM analysis coincide with the results of the XRD analysis. SAED pattern in Fig. 4(b) demonstrated concentric rings with intermittent dots which indicated that the synthesized nanoparticle was crystalline. The parti-

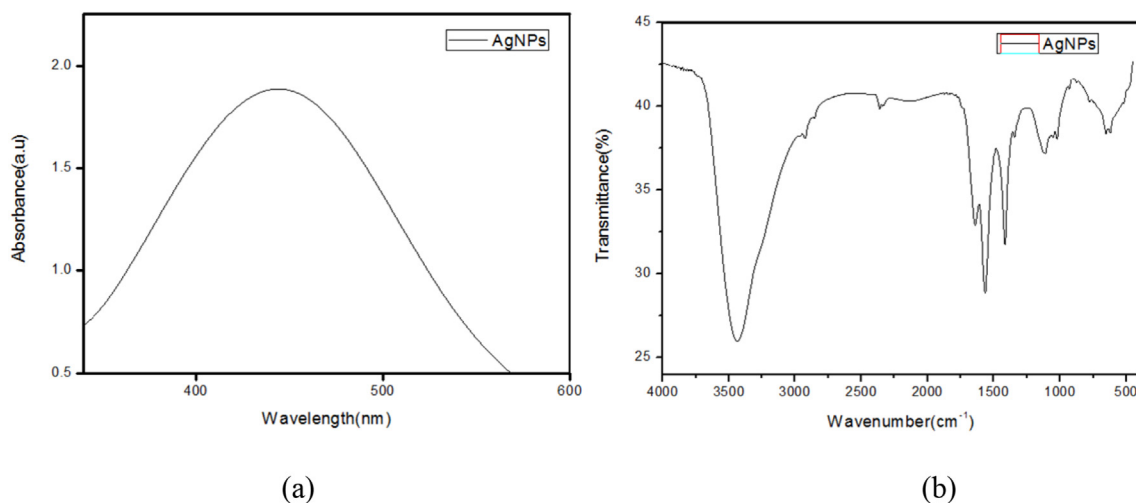


Fig. 2. (a) UV-Vis spectrum and (b) FTIR spectrum of AgNPs synthesized using *F. incarnatum* fungal extract.

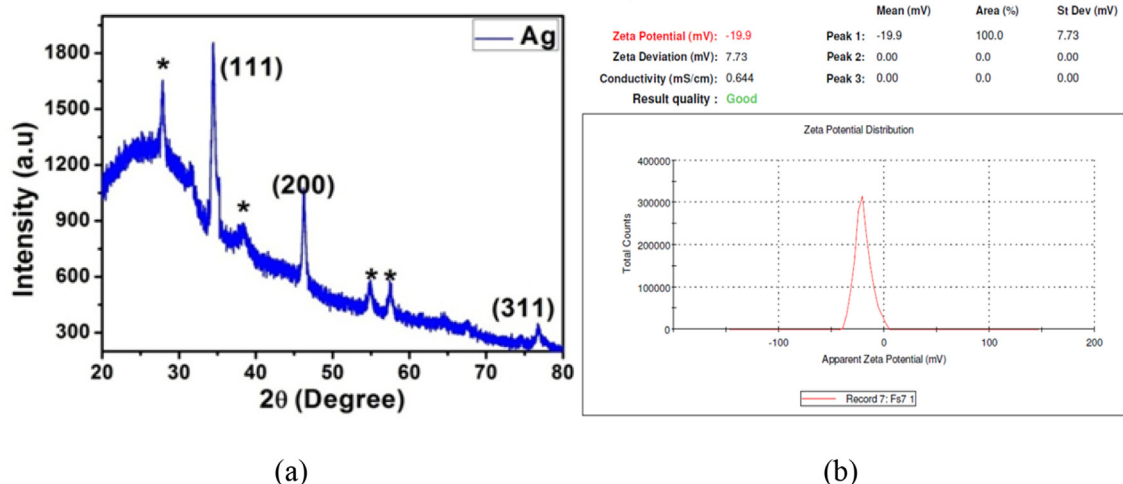


Fig. 3. (a) XRD pattern and (b) Zeta potential analysis of AgNPs synthesized using *F. incarnatum* fungal extract.

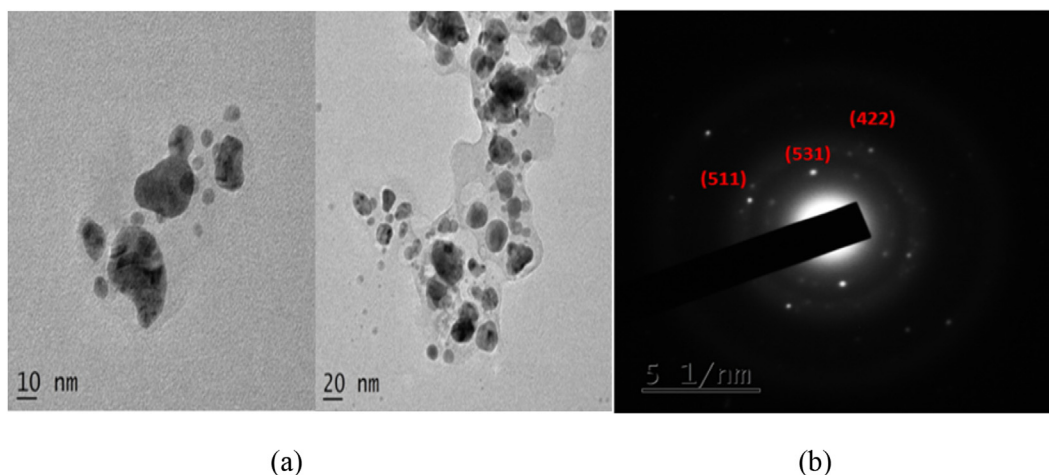


Fig. 4. (a) HR-TEM micrograph and (b) SAED pattern of AgNPs synthesized using *F. incarnatum* fungal extract.

cle size of AgNPs synthesized using *Penicillium diversum* ranged between 5 and 30 nm (Singh et al., 2014). Whereas Raheman et al., reported the AgNPs size ranged from 10 to 40 nm. Comparatively the AgNPs size synthesized in the present study was smaller which is possibly due to the different proteins present in the fungal extract and the optimization parameters.

3.4. Antibacterial activity

The potency of the *Fusarium* was evaluated by antibacterial activity. Mycosynthesized AgNPs showed potent antibacterial activity against *E. coli* (12.2 mm) and *S. aureus* (11 mm) zone of inhibition was observed. The nanoparticles released silver ions in the bacterial cells which helped to increase the antibacterial activity, and also inhibit the growth of both gram-positive and gram-negative bacteria. It was noted that even low concentration nanoparticles inhibit the growth of bacteria which shows a good antibacterial property (Wang et al., 2017). The attraction of AgNPs depended on the particle surface area; a small size nanoparticle will offer a greater surface area which will give a significant microbial activity. AgNPs can bind fast to the bacterial cell wall and lead to structural changes and finally cell death (Nallal et al., 2021).

3.5. Cytotoxicity determination of optimized AgNPs on SK-MEL-3 cells

Studies have shown that the cytotoxic effect of AgNPs depends on the size and concentration of the nanoparticles. Depending on the surface alterations brought about by the extract used for the synthesis the toxicity of the AgNPs may differ greatly (Abdel-Aziz et al., 2014). The percentage of cell growth inhibition increased as the concentration of AgNPs increased, according to the MTT assay results. Cell viability was demonstrated to be done dependent. The cytotoxicity effect of the AgNPs on SK-MEL-3 cells can be visualized from the morphological changes. AgNPs showed effective anticancer activity at lower concentrations with an IC₅₀ value of 17.70 µg/ml. Notably, an IC₅₀ value of 250 µg/ml and 18.50 µg/ml was obtained for *F. incarnatum* fungal extract and standard Kojic acid. Interestingly, the concentration of AgNPs required to inhibit human skin melanoma cells were lower when compared to the concentration of standard Kojic acid. Detachment, shrinking, and membrane blabbing were visible morphological alterations and finally results in the disintegration of cell structure, Fig. 5. AgNPs synthesized using *F. semitectum* inhibited human gingival fibroblast (HGF) cells at a CTC₅₀ concentration of 260 µg/ml (Halkai et al., 2019). This suggests that fungi of the *Fusarium* genus

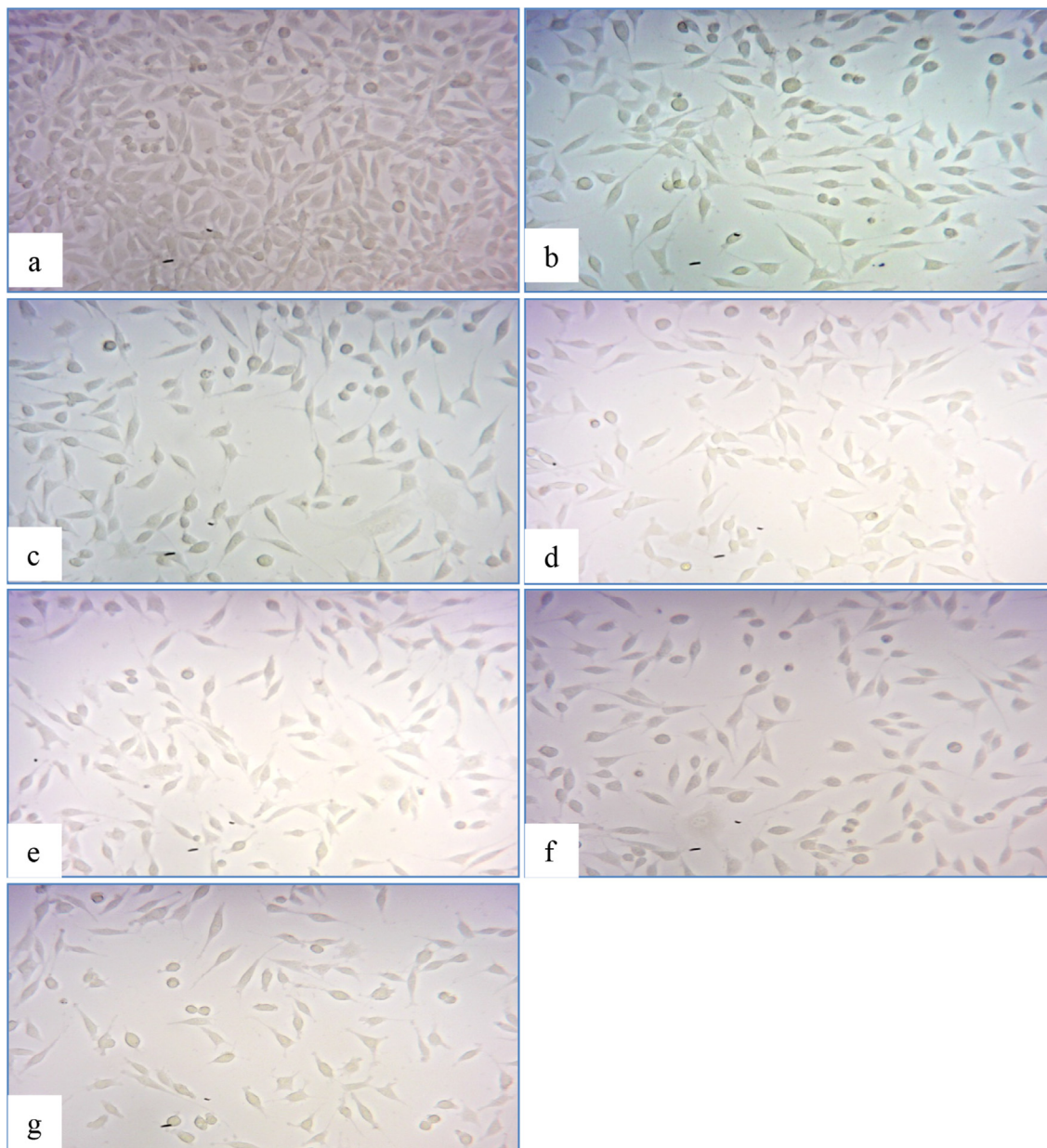


Fig. 5. In-vitro cytotoxicity assay photomicrographs of SK-MEL-3 cancer cell lines: (a) intact control cells, (b) 200 µg of extract, (c) 250 µg of extract, (d) 15 µg Kojic acid, (e) 20 µg of Kojic acid, (f) 10 µg AgNPs and (g) 15 µg AgNPs.

are eminent resources for the synthesis of AgNPs with superior cytotoxic activity against cancerous cells.

3.6. Cellular Tyrosinase activity

Tyrosinase is the main enzyme in the biosynthesis of melanin. Cellular Tyrosinase assay was performed to evaluate the Tyrosinase inhibition efficiency of *F. incarnatum* fungal extract, optimized AgNPs and standard Kojic acid in human skin melanoma SK-MEL-3 cells. The efficiency of optimized AgNPs increased with the increase in concentration suggesting that cellular tyrosinase inhibition was dose-dependent [Table 1](#). The IC_{50} value of 32.60 µg/ml was obtained for optimized AgNPs, whereas the IC_{50} value of *F. incarnatum* extract and standard Kojic acid was 446.2 µg/ml & 33.3 µg/ml after 72 h of incubation. Optimized AgNPs synthesized from *F. incarnatum* extract showed efficient cellular Tyrosinase

Table 1
Cell Tyrosinase activity on SK-MEL-3 Human Skin Melanoma Cells.

S.No	Sample	Viable cells (%)
1	Control	100.05 ± 7.6
2	Fungal extract (200 µg)	70.6 ± 5.36
3	Fungal extract (250 µg)	27.12 ± 2.06
4	AgNPs (10 µg)	68.03 ± 5.2
5	AgNPs (15 µg)	23.02 ± 1.75
6	Kojic acid (15 µg)	48.3 ± 3.6
7	Kojic acid (20 µg)	30.1 ± 2.28

inhibition activity when compared to the fungal extract and standard Kojic acid suggesting the potent melanin suppressing ability of the optimized AgNPs. *Pistacia vera* shell extract was highly effective in suppressing cellular Tyrosinase activity at a concentration of 0.5 mg/ml ([Sarkhail et al., 2017](#)) which supports our result that the concentration of crude extract is required in higher concentration,

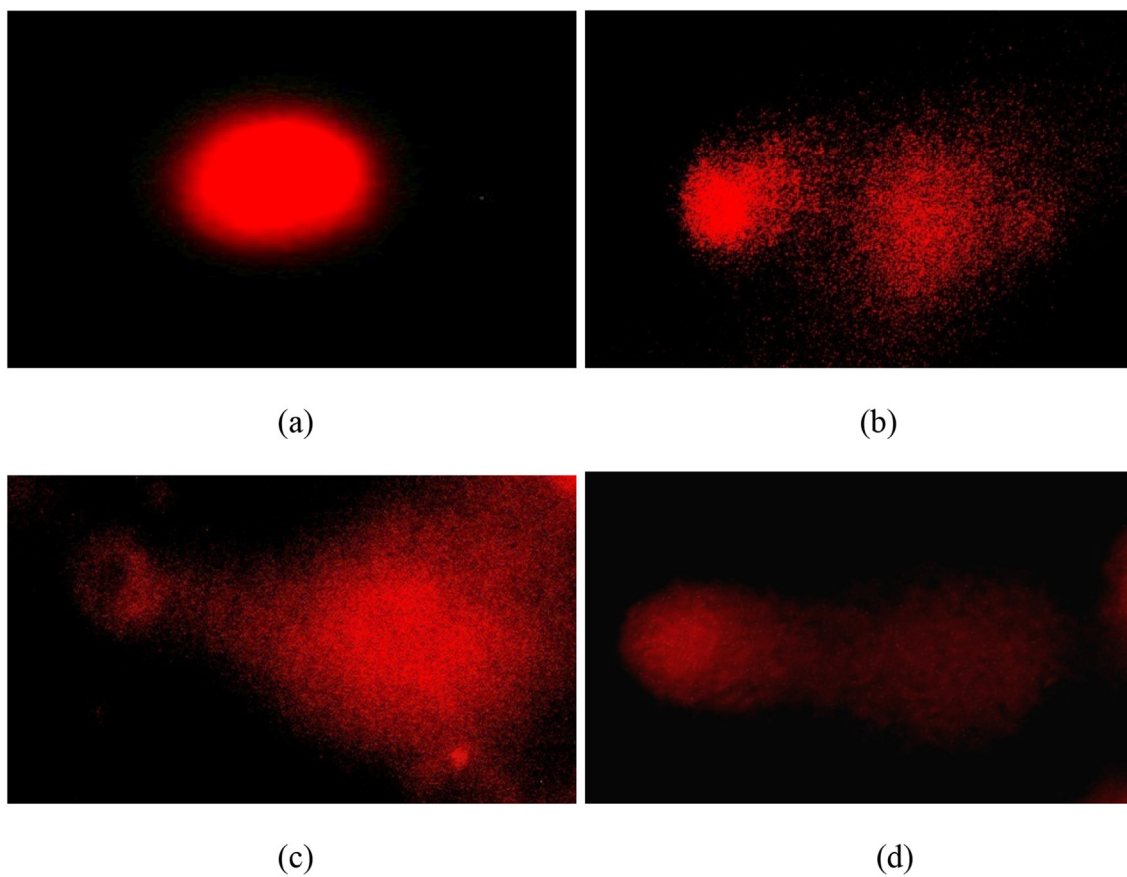


Fig. 6. Alkaline single gel electrophoresis Comet assay (a) intact SK-MEL-3 control cells, (b) SK-MEL-3 cells treated with 250 µg of *F. incarnatum* fungal extract (c) SK-MEL-3 cells treated with 20 µg of Kojic acid, (d) SK-MEL-3 cells treated with 15 µg of AgNPs.

whereas, AgNPs are highly efficient in suppressing Tyrosinase enzyme at a low concentration. Moreover, the results revealed that the obtained IC₅₀ concentration of optimized AgNPs can be considered as a non-lethal dose with potent tyrosinase and demelanization activity.

3.7. DNA fragmentation

The impact of AgNPs, fungal extract and Kojic acid treatment on human skin melanoma SK-MEL-3 cells was examined using alkaline single cell gel electrophoresis assay. SCGE is an extremely sensitive technique for determining the extent of DNA damage in eukaryotic cells (Nandhakumar et al., 2011). Results of this assay revealed that the control cells remained intact indicating undamaged DNA associated with matrix protein inside the nucleus. Fragmentation was observed for the cells treated with fungal extract, AgNPs and Kojic acid indicating DNA damage Fig. 6. Brighter and longer tails were observed in cells treated with 15 µg of AgNPs synthesized using *F. incarnatum* fungal extract. The signals of DNA damage in cells treated with Kojic acid were similar to AgNPs treatment but at higher concentrations. Fungal extract treatment caused impressive DNA damage as observed in the photomicrographs but at a concentration of 250 µg/ml. AgNPs were efficient in causing DNA damage to the cells when compared to the positive control and crude fungal extract.

4. Conclusion

The bio-fabrication of metallic nanoparticles using fungal extracts is considered a novel and prominent approach in the field

of sustainable nanotechnology. Among the numerous fungal species *Fusarium* spp. have gained special attention for the biosynthesis of nanoparticles since this approach is appreciably eco-friendly and cost-effective using simple methods. The present study highlights the biosynthesis of spherical AgNPs from *F. incarnatum* fungal extract with an average particle size of 4 nm and demonstrates the effective antimicrobial activity and impressive anti-melanogenic activity of synthesized AgNPs on SK-MEL-3 human skin melanoma cells at a very low concentration suggesting it as a potential candidate to be explored in pharmaceutical industries.

Conflict of interest

The authors have no conflicts of interest.

Acknowledgement

The authors extend their appreciation to the Researchers supporting Project number (RSP-2021/393) King Saud University, Riyadh, Saudi Arabia.

References

- Abdel-Aziz, M.S., Shaheen, M.S., El-Nekeety, A.A., Abdel-Wahhab, M.A., 2014. Antioxidant and antibacterial activity of silver nanoparticles biosynthesized using *Chenopodium murale* leaf extract. *J. Saudi Chem. Soc.* 18, 356–363.
- AbdelRahim, K., Mahmoud, S.Y., Ali, A.M., Almaary, K.S., Mustafa, A.-Z., Hussein, S.M., 2017. Extracellular biosynthesis of silver nanoparticles using *Rhizopus stolonifer*. *Saudi J Biol Sci.* 24, 208–216.
- Azmah, P., Baker, S., Rakshith, D., Satish, S., 2016. Mycosynthesis of silver nanoparticles bearing antibacterial activity. *Saudi Pharm. J.* 24, 140–146.

- Balaji, D.S., Basavaraja, S., Deshpande, R., Mahesh, D.B., Prabhakar, B.K., Venkataraman, A., 2009. Extracellular biosynthesis of functionalized silver nanoparticles by strains of *Cladosporium cladosporioides* fungus. *Colloids Surf. B* 68, 88–92.
- Birla, S.S., Gaikwad, S.C., Gade, A.K., Rai, M.K., 2013. Rapid Synthesis of silver nanoparticles from *Fusarium oxysporum* by optimizing physicochemical conditions. *Sci. World J.* 2013, 1–12.
- Delgado, Y., Martinez, C.E., Cortez, M., Flores, N.S., Flores, M., 2018. Optical properties of silver, silver sulfide and silver selenide nanoparticles and antibacterial applications. *Mater. Res. Bull.* 99, 385–392.
- Deshmukh, S.P., Patil, S.M., Mullani, S.B., Delekar, S.D., 2019. Silver nanoparticles as an effective disinfectant: a review. *Mat. Sci. Eng. C-Mater.* 97, 954–965.
- Dutta, T., Chattopadhyay, A.P., Ghosh, N.N., Khatua, S., Acharya, K., Kundu, S., Mitra, D., Das, M., 2020. Biogenic silver nanoparticle synthesis and stabilization for apoptotic activity; insights from experimental and theoretical studies. *Chem. Pap.* 74, 4089–4101.
- Ganachari, S.V., Bhat, R., Deshpande, R., Venkataraman, A., 2012. Extracellular biosynthesis of silver nanoparticles using fungi *Penicillium diversum* and their antimicrobial activity studies. *Bio. NanoSci.* 2, 316–321.
- Halkai, K.R., Mudda, J.A., Shivanna, V., Patil, V., Rathod, V., Halkai, R., 2019. Cytotoxicity evaluation of fungal-derived silver nanoparticles on human gingival fibroblast cell line: an in vitro study. *J. Conserv. Dent.* 22, 160–163.
- Himalini, S., Razia, M., 2019. Nutrient analysis of agriculture and forest soils in high altitude of Kodaikanal. *Nat. Environ. Pollut. Technol.* 18, 619–662.
- Kalishwaralal, K., Deepak, V., Ramkumarandian, S., Nellaiah, H., Sangiliyandi, G., 2008. Extracellular biosynthesis of silver nanoparticles by the culture supernatant of *Bacillus licheniformis*. *Mater. Lett.* 62, 4411–4413.
- Kathiresan, K., Manivannan, S., Nabeel, M.A., Dhivya, B., 2009. Studies on silver nanoparticles synthesized by a marine fungus, *Penicillium fellutanum* isolated from coastal mangrove sediment. *Colloids Surf.* 71, 133–137.
- Konstantinov, N.K., Ulf-Møller, C.J., Dimitrov, S., 2016. Histone variants and melanoma: facts and hypotheses. *Pigment Cell Res.* 29, 426–433.
- Laikova, K.V., Oberemok, V.V., Krasnodubets, A.M., Gal'chinsky, N.V., Useinov, R.Z., 2019. Advances in the understanding of skin cancer: ultraviolet radiation, mutations, and antisense oligonucleotides as anticancer drugs. *Molecules* 24, 1516.
- Lalitha, A., Subbaiya, R., Ponmurugan, P., 2013. Green synthesis of silver nanoparticles from leaf extract *Azadirachta indica* and to study its anti-bacterial and antioxidant property. *Int. Curr. Microbiol. Appl. Sci.* 2, 228–235.
- Lee, S.H., Jun, B.H., 2019. Silver nanoparticles: synthesis and application for nanomedicine. *Int. J. Mol. Sci.* 20, 865.
- Malik, P., Shankar, R., Malik, V., Sharma, N., Mukherjee, T.K., 2014. Green chemistry based benign routes for nanoparticle synthesis. *J. Nanopar.* 2014, 1–14.
- Nallal, V.U.M., Prabha, K., VethaPotheher, I., Ravindran, B., Baazeem, A., Chang, S.W., Otunola, G.A., Razia, M., 2021. Sunlight-driven rapid and facile synthesis of silver nanoparticles using *Allium ampeloprasum* extract with enhanced antioxidant and antifungal activity. *Saudi J. Biol. Sci.* 28, 3660–3668.
- Nandhakumar, S., Parasuraman, S., Shanmugam, M.M., Rao, K.R., Chand, P., Bhat, B. V., 2011. Evaluation of DNA damage using single-cell gel electrophoresis (Comet Assay). *JPP* 2, 107–111.
- Ninganagouda, S., Vandana, R., Jyoti, H., Singh, D., Kulkarni, P., 2013. Extracellular biosynthesis of silver nanoparticles using *Aspergillus Flavus* and their antimicrobial activity against gram negative MDR strains. *Int. J. Pharm. Bio. Sci.* 4, 222–229.
- Othman, A.M., Elsayed, M.A., Al-Balakocy, N.G., Hassan, M.M., Elshafei, A.M., 2019. Biosynthesis and characterization of silver nanoparticles induced by fungal proteins and its application in different biological activities. *JEGB* 17, 8.
- Prabhu, S., Poulouse, E.K., 2012. Silver nanoparticles: mechanism of antimicrobial action, synthesis, medical applications, and toxicity effects. *Int. Nano Lett.* 2, 1–10.
- Raheman, F., Deshmukh, S., Ingle, A., Gade, A., Rai, M., 2011. Silver nanoparticles: novel antimicrobial agent synthesized from an endophytic fungus *Pestalotia* sp. isolated from leaves of *Syzygium cumini* (L). *Nano Biomed. Eng.* 3, 174–178.
- Rajendran, P., Maheshwari, U., Muthukrishnan, A., Muthuswamy, R., Anand, K., Ravindran, B., Dhanaraj, P., Balamuralikrishnan, B., Chang, S.W., Chung, W.J., 2021. Myricetin: versatile plant based flavonoid for cancer treatment by inducing cell cycle arrest and ROS-reliant mitochondria-facilitated apoptosis in A549 lung cancer cells and in silico prediction. *Mol. Cell. Biochem.* 476, 57–68.
- Rigel, D.S., Russak, J., Friedman, R., 2010. The evolution of melanoma diagnosis: 25 years beyond the ABCDs. *CA Cancer J. Clin.* 60, 301–316.
- Roy, S., Das, T., 2014. Biosynthesis of silver nanoparticles by *Aspergillus foetidus*: optimization of physicochemical parameters. *Nanosci. Nanotechnol. Lett.* 6, 181–188.
- Salem, W., Leitner, D.R., Zingl, F.G., Schratte, G., Prassl, R., Goessler, W., Reidl, J., Schild, S., 2015. Antibacterial activity of silver and zinc nanoparticles against *Vibrio cholerae* and enterotoxigenic *Escherichia coli*. *Int. J. Med. Microbiol.* 305, 85–95.
- Sarkhail, P., Salimi, M., Sarkheil, P., Kandelous, M.H., 2017. Anti-Melanogenic activity and cytotoxicity of pistacia vera hull on human melanoma SKMEL-3 cells. *Acta Med. Iran* 55, 422–428.
- Sastry, M., Ahmad, A., Khan, M.I., Kumar, R., 2004. Microbial nanoparticle production. In: Niemeyer CM, Mirkin CA (ed). *Nanobiotechnology*. Wiley-VCH Verlag GmbH & Co., Weinhei. 29, 126–135.
- Shankar, S.S., Rai, A., Ahmad, A., Sastry, M., 2004. Rapid synthesis of Au, Ag, and bimetallic Au core-Ag shell nanoparticles using Neem (*Azadirachta indica*) leaf broth. *J. Colloid Interf. Sci.* 275, 496–502.
- Siddiqi, K.S., Husen, A., Rao, R., 2018. A review on biosynthesis of silver nanoparticles and their biocidal properties. *J. Nanobiotechnol.* 16, 14.
- Singh, S., Bharti, A., Meena, V., 2014b. Structural, thermal, zeta potential and electrical properties of disaccharide reduced silver nanoparticles]. *Mater. Sci.: Mater. Electron.* 25, 3747–3752.
- Singh, D., Rathod, V., Ninganagouda, S., Hiremath, J., Singh, A.K., Mathew, J., 2014a. Optimization and characterization of silver nanoparticle by endophytic fungi *Penicillium* sp. isolated from *Curcuma longa* (Turmeric) and application studies against MDR *E. coli* and *S. aureus*. *Bioinorg. Chem. Appl.* 2014, 1–8.
- Thakkar, K.N., Mhatre, S.S., Parikh, R.Y., 2010. Biological synthesis of metallic nanoparticles. *Nanomedicine* 6, 257–262.
- Veerasamy, R., Xin, T.Z., Gunasagaran, S., Xiang, T.F.W., Yang, E.F.C., Jeyakumar, N., Dhanaraj, S.A., 2011. Biosynthesis of silver nanoparticles using mangosteen leaf extract and evaluation of their antimicrobial activities. *J. Saudi Chem. Soc.* 15, 113–120.
- Wang, L., Hu, C., Shao, L., 2017. The antimicrobial activity of nanoparticles: present situation and prospects for the future. *Int. J. Nanomed.* 12, 1227–1249.
- Wozniak, K., Czechowska, A., Blasiak, J., 2004. Cisplatin-evoked DNA fragmentation in normal and cancer cells and its modulation by free radical scavengers and the tyrosine kinase inhibitor ST1571. *Chem-Biolo Interac.* 147, 309–318.
- Zada, S., Ahmad, A., Khan, S., 2018. Biofabrication of gold nanoparticles by *Lyptolyngbya* JSC-1 extract as super reducing and stabilizing agents: synthesis, characterization and antibacterial activity. *Microb. Pathog.* 114, 116–123.